SHEAR LOCALIZATION-MARTENSITIC TRANSFORMATION INTERACTIONS IN Fe-Cr-Ni MONOCRYSTAL

B. Y. Cao[1], M. A. Meyers[1], V. F. Nesterenko[1], D. Benson[1], and Y.B. Xu[2]
[1] *University of California, San Diego, La Jolla, CA 92093,*
[2] *Institute of Metal Research, Chinese Academy of Sciences, Shenyang 110016, P. R. China*

Abstract. A Fe-15wt%Cr-15wt%Ni alloy monocrystal was deformed dynamically (strain rate~$10^4 s^{-1}$) by the collapse of an explosively driven thick-walled cylinder under prescribed temperature and strain. The experiments were carried out under the following conditions: (a) Alloy in austenitic state; (b) Alloy in transformed state; (c) Alloy at temperature slightly above M_s. The last case is characterized by precipitating concurrent shear-band propagation and martensitic transformation. The alloy exhibited profuse shear-band formation depending on the deformation condition. Stress-assisted and strain-induced martensitic transformation competed with shear localization. The alloy that was deformed at a temperature slightly above M_s showed a significantly reduced number of shear bands. The anisotropy of plastic deformation determined the evolution of strains and distribution of shear bands. Calculated shear-band spacings based on the Grady-Kipp and Wright-Ockendon theories are compared with observed values. The microstructure within shear bands was characterized by transmission electron microscopy. Regions of sub-micron grain sizes exhibiting evidence of recrystallization were observed, as well as amorphous regions possibly resulting from melting and rapid resolidification of heavily deformed material inside shear band.

INTRODUCTION

Shear localization is an extreme case of inhomogeneous deformation where plastic deformation localizes in a thin region of a specimen. In most cases, shear localization is associated with a local softening of the material. This softening can be due to thermal or geometrical reasons, or due to microfracture.

In thermal softening, the local increase in temperature leads to localization. In the extreme case when the strain rate is so high that the generated local heat cannot escape from the deformation area, shear bands are formed, which are called "adiabatic". Regardless of the initial softening mechanism, the localized deformation leads to an accelerated strain rate. Eventually, there are heat concentration and thermal effects in most situations [1,2].

Nesterenko, Meyers and co-workers [3-5] have established that shear bands in metals organize themselves with a characteristic spacing that is a function of material parameters; it was found that this spacing evolves with the development of the shear bands, so that smaller shear bands have a smaller spacing.

The goal of this research was to determine the interaction between shear localization and martensitic transformation.

EXPERIMENTAL METHODS

The FCC alloy Fe-15wt%Cr-15wt%Ni was chosen for this investigation because it has a very well characterized deformation and transformation response. A monocrystalline cylindrical specimen with 32 mm diameter was grown at the Advanced Research and Development Laboratory at Pratt and

CP706, *Shock Compression of Condensed Matter - 2003,* edited by M. D. Furnish, Y. M. Gupta, and J. W. Forbes

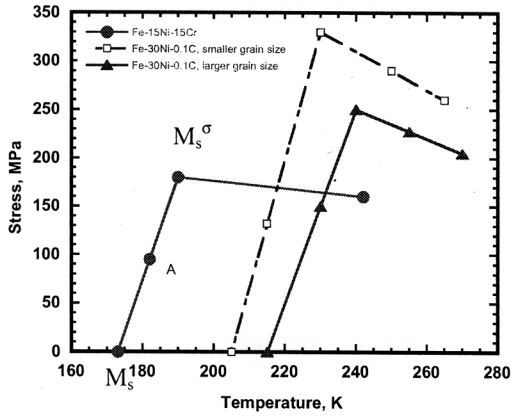

FIGURE 1. Temperature dependence of the material yield strength for Fe-15Cr-15Ni: Fe-15Cr-15Ni, M_s=173 K (data from Stone &Thomas [6] and Guimaraes et al. [7], D = 0.211mm; D = 0.101mm.

Whitney Aircraft. This alloy was homogenized at 1,500K for 72 hours. Figure 1 shows the estimated M_s temperature for this alloy, obtained by using point A (182 K, 80 MPa [6]) and an assumed slope of the stress-assisted range. For comparison, the measured results for Fe-30Ni-1C [7] at two grain sizes (D) are shown in the same plot. The reduction of grain size affects the M_s temperature.

The dynamic method of plastic deformation used in this investigation, the collapsing thick-walled cylinder, has been used and thoroughly characterized for multiple shear band generation [8]. The thick-walled cylinder (TWC) implosion technique was introduced by Nesterenko and Bondar [9] and represents an improvement from the confined exploding cylinder technique developed by Shockey [10].

In TWC test, the specimen is sandwiched between a copper driver tube and a copper stopper tube and is collapsed inward during the test. Figure 2(a) shows the initial and imploded configurations. OFHC copper was used to make these tubes. The internal diameters of the inner copper tube were selected to produce prescribed and controlled final strains. In some special cases, a central steel rod was also used. The explosive is axi-symmetrically placed around the specimen (Fig. 2(b)). The detonation is initiated on the top. The expansion of the detonation products exerts a uniform pressure on the cylindrical specimen and drives the specimen to collapse inward. The detonation velocity of the selected explosive is approximately 4000 m/s and its density is 1 g/cm^3. The velocity of the inner wall of the tube was determined by an electromagnetic gage [9].

The conditions for the three experiments were:

1. $T < M_s$: alloy in martensitic state; test was conducted at 190 K. The sample was first cooled down to the 77 K. After that, temperature was raised to 190 K, when explosive charge was detonated.
2. $M_s < T < M_s^\sigma$: concurrent deformation and transformation. Experiment conducted at 188 K (-850 C).
3. $T > M_s^\sigma$: no transformation. Experiment was conducted at 273 K.

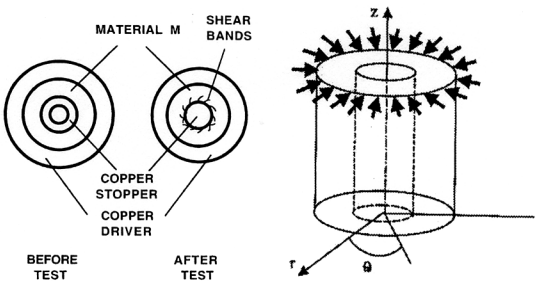

FIGURE 2. Thick-Walled Cylinder Test.

RESULTS AND DISCUSSION

Figure 3 shows the differences in collapse geometry between monocrystalline Fe-15%Cr-15%Ni (Fig. 3(a)) and polycrystalline AISI 304 stainless steel (Fe-18%Cr-8%Ni) (Fig. 3(c)). The crystallographic anisotropy creates a global mechanical anisotropy in the monocrystal. This results in a difference in resistance to the collapse. Stone and Thomas [6] show the stress strain response obtained for the [001] and [011] directions.

The Fe-Cr-Ni monocrystal has a response characteristic of FCC monocrystals: the [001] orientation has four slip systems with identical Schmid factors and therefore a higher yield stress. Thus, the [001] direction shows a greater resistance to collapse. This symmetry is revealed by the tendency of the cylinder to become square.

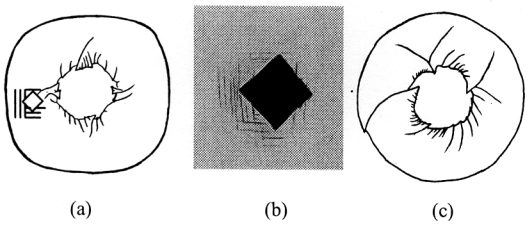

FIGURE 3. Configuration of shear bands in specimen subjected to implosion with ε_{eff} = 0.92: (a) in Fe-15Cr-15Ni monocrystal: cylinder axis: [100]; (b) Microhardness indentation and traces of [111] slip planes (the traces are [110] orientation); (c) Polycrystalline Fe-18Cr-8 Ni.

The number of shear bands formed was also affected by the conditions of deformation. The untransformed and pre-transformed conditions showed a large number of shear bands (N_s equal to 41 and 56, respectively). If transformation was active during deformation, then a marked decrease in the number of shear bands: N_s=10, was observed. This drastic reduction is the direct result of the competition between shear localization and martensitic transformation in the process of strain accommodation. The decrease in the number of shear bands and the associated increase in their spacing can be explained, partially, by the reduced yield stress. Both Grady-Kipp [11] and Wright-Ockendon-Molinari [12,13] analyses predict an inverse relation between yield stress and shear-band spacing. The corresponding equations can be expressed as:

$$\text{Grady} - \text{Kipp} \qquad L = 2\pi\left[\frac{kC}{\dot{\gamma}^3 a^2 \tau_0}\right]^{1/4} \cdot \frac{9^{1/4}}{\pi}, \qquad (1)$$

$$\text{Wright} - \text{Ockendon} \qquad L = 2\pi\left[\frac{kC}{\dot{\gamma}^3 a^2 \tau_0}\right]^{1/4} \cdot m^{3/4}, \qquad (2)$$

$$\text{Molinari} \qquad L = 2\pi\left[\frac{kC}{\dot{\gamma}^3 \tau_0 a^2}\right]^{1/4} \cdot \left[\frac{m^3(1-aT_0)^2}{(1+m)}\right]^{1/4}, \qquad (3)$$

where the heat capacity is C = 500 J/KgK, thermal conductivity K = 14.7 W/mK, thermal softening factor a = 7.2 x 10^{-4} K^{-1}, strain rate hardening index

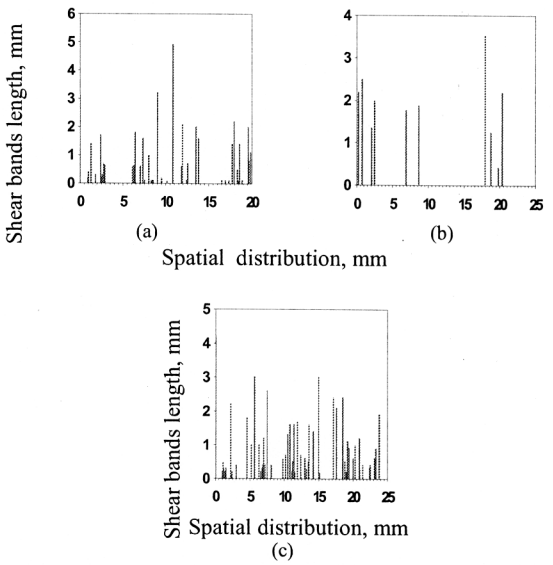

FIGURE 4. Shear bands distributions in three specimens deformed at: (a) Ambient temperature-no transformation; (b) 188 K, simultaneous transformation; (c) Pre-transformed structure.

m = 0.026, and shear strain rate $\dot{\gamma}$ = 6 x 10^4[8].

These models predict an increase in the spacing by 50%, if yield stress is reduced by 80%. The difference in the experimental results is much more dramatic, as shown by the quantitative measurements in Figure 4. The spacing of shear bands was calculated assuming that they initiated at a strain of 0.1. The spacing in the condition undergoing simultaneous transformation and deformation (L=4.03 mm) is about four times the spacings for the other conditions (L=0.98 mm and L=0.72 mm). This test was carried out at 188 K; the shear yield stress is reduced from 90 MPa to 50 MPa.

The analysis of the microstructure reveals important features. The austenitic monocrystal had a pattern of gray crisscrossing regions. These regions are diffuse and indicate that the composition of the alloy is not entirely homogeneous. The pre-transformed material shows shear bands cutting through the pre-existing martensite. Figure 5 shows the microstructure of the material imploded at 188 K. We can see the existence of stress-assisted/strain-induced martensite as well as shear localization. Fig.

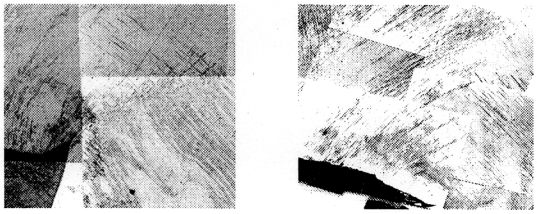

(a) (b)

FIGURE 5. Martensite transformation during deformation (Fe-15Cr-15Ni collapsed cylinder at T=188 K); (a) Interaction of shear bands and stress-assisted martensite; (b) Region along internal surface where deformation was accommodated by martensite transformation.

5(a) shows one principal shear band and several martensite laths forming at its tip, in a fan-like pattern. Fig. 5(b) shows a region along the surface in which the plastic deformation was accommodated by transformation. Several laths can be seen, emanating from the surface. No shear bands were formed in this region.

Transmission electron microscopy was conducted inside the shear band. The features revealed are identical to the ones seen for a polycrystalline AISI 304 stainless steel. In general, an equiaxed structure with grains in the range of 100-300 nm was observed. This is shown in Figure 6. The formation of sub-micrometer grains has been attributed to a rotational dynamic recrystallization process [14]. Fig. 6 also shows an amorphous region. The formation of the amorphous region is thought to be due to melting and very high rate resolidification. A similar

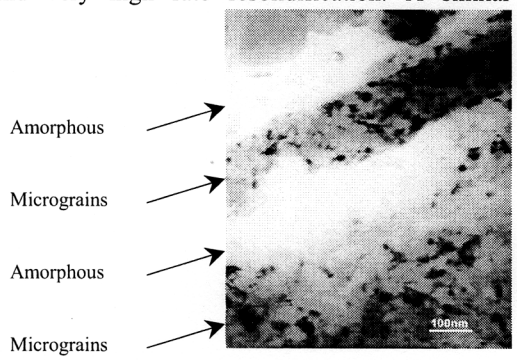

FIGURE 6. TEM of shear band shows microcrystalline and amorphous regions in Fe-15wt%Cr-15wt%Ni.

microstructure has been seen earlier by Meyers et al. [14] for AISI stainless steel. However, this was only possible for higher carbon concentrations. The cooling rate inside the shear band is extremely high and could possibly lead to melting and resolidification in the glassy state. We can estimate the cooling rate $\dot{T} = \frac{T_m}{\tau}$, where $\tau \sim \frac{\delta^2}{D}$, thickness of shear bands δ, thermo-diffusivity D. In our case, $\dot{T} \sim 4 \times 10^9 \, K/s$.

ACKNOWLEDGMENT

We would like to thank Dr. S. Usherenko, Dr. D. Lassila, Dr. Q. Xue and Professor G. Stone.

REFERENCES

1. Rogers, H. C., *Annu. Rev. Mater. Sci.*, **2,** 283 (1979).
2. Nesterenko, V. F., *Dynamics of Heterogeneous Materials,* Spinger-Verlag, NY, 2001, pp. 307-384.
3. Nesterenko, V. F., Meyers, M. A., and Chen, H. C., *Acta Metall.* **44,** 2017 (1996).
4. Nesterenko, V. F., Meyers, M. A., LaSalvia, J. C., Bondar, M. P., Chen, Y. J., and Lukyanov, Y. L., *Mater. Sci. Eng.* A, **229**, 23 (1997).
5. Nesterenko, V. F., Meyers, M. A., and Wright, T. W., *Acta Mater.* **46,** 327 (1998).
6. Stone, G., and Thomas, G., *Metall. Trans.* **5**, 2095 (1974).
7. Guimaraes, J.R.C., Gomes, J.C., and Meyers, M.A., *Suppl. Trans. J. I. M.,* **17**, 411 (1976)
8. Xue, Q., Nesterenko, V.F., and Meyers, M.A., *International Journal of Impact Engineering,* **28**, 257 (2003).
9. Nesterenko, V.F., and Bondar, M. P., *DYMAT Journal*, **1,** 245 (1994).
10. Shockey, D.A., In *Metallurgical Applications of Shock-Wave and High-Strain-Rate Phenomena*, edited by Murr, L.E., Staudhammer, K.P., and Meyers, M.A., Dekker, NY, 1986, pp. 633-656.
11. Grady, D.E., and Kipp, M.E., *J. Mech. Phys. Solids,* **35**, 95 (1987).
12. Wright, T. W., and Ockendon, H., *Int. Journal of Plasticity,* **12**, 927 (1996).
13. Molinari, A., *J. Mech. Phys. Solids*, **45,** 1551 (1997).
14. Meyers, M. A., Xu, Y. B., Xue, Q., Perez-Prado, M. T., and McNelley, T. R., *Acta Mat.*, **51**, 1307 (2003).